

SIMULATION OF THE DRYING CHARACTERISTICS OF GROUND NEEM SEEDS IN A FLUIDISED BED

A. KUYE^{1*}, C. O. C. OKO², S. N. NNAMCHI¹

¹Department of Chemical Engineering

²Department of Mechanical Engineering

University of Port Harcourt, PMB 5323, Port Harcourt, NIGERIA.

*Corresponding Author: aokuye@enguniport.org

Abstract

The neem seed is a good source of neem oil as well as insecticides and pesticides. The oil and insecticides can be extracted by two consecutive leaching of neem seed kernels with hexane and ethanol. This work presents a model for simulating the drying of neem seeds in a fluidized bed. Experimental values obtained from literature were used to validate the model prediction. The drying simulation results show that there was a good agreement between the experimental values and the corresponding model predictions.

Keywords: Simulation, Neem seeds, Fluidized bed dryer.

1. Introduction

Neem seeds are extracted from neem tree (*Azadirachta indica A. Juss*) and are rich in neem oil as well as insecticides and pesticides. The seed kernels contain 40 to 50% by mass of non-edible oil and 20% of biodegradable substances that are active against a wide variety of pests [1]. In a typical manufacturing process, the oil and insecticides are removed by two consecutive leaching of neem seed kernels with organic solvents. Hexane is first used to remove oil from the seed, thereafter; ethanol is used to extract the insecticide from the de-oiled seeds [2].

Nomenclatures

A_s	Total surface area of particles m^2
C_{BLM}	Mean logarithmic molar concentration of the dry air $kmol/m^3$
C_p	Specific heat capacity $kJ/kg\ K$
C_T	Total molar concentration $kmol/m^3$
df	Degree of freedom
d_s	Particle diameter m
f	Normalized drying rate
g	Gravitational acceleration m/sec^2
G	Gas flow kg/sec
H	Enthalpy kJ/kg
h_c	Heat transfer coefficient $kW/m^2\ K$
h_D	Mass transfer coefficient m/sec
k	Thermal conductivity W/mK
k'	Drying rate constant Sec^{-1}
M	Molecular weight $kg/kmol$
m_s	Dry solid mass kg
N_{TG}	Number of gas transfers in the bed.
Nu	Nusselt number
N_v	Drying rate per surface of solid $kg/m^2\ sec$
N_{v0}	Initial drying rate per surface of solid $kg/m^2\ sec$
N_w	Drying rate during constant rate period $kg/m^2\ sec$
Pr	Prandtl number
P	Total pressure KPa
q_c	Heat flux $kJ/m^2\ secK$
Re	Reynolds number
Sc	Schmidt number
T	Temperature K
t	Time sec
u	Gas velocity m/sec
VP	Vapour pressure KPa
X	Solvent content of the solid kg/kg
Y	Solvent content of the gas kg/kg
y	Molar fraction of solvent $kmol/kmol$
<i>Greek Symbols</i>	
μ	Viscosity $Pa.s$
ρ	Density Kg/m^3
λ	Latent heat of vapourisation J/kg
<i>Subscripts</i>	
0	Auperficial, initial condition
Amb	Ambient
$calc$	Calculated
$crit$	Critical
E	Equilibrium

<i>Eth</i>	Ethanol
<i>exp</i>	Experimental
<i>g</i>	Gas
<i>Hex</i>	Hexane
<i>i</i>	Interfacial
<i>liq</i>	Liquid
<i>max</i>	Maximum
<i>min</i>	Minimum
<i>out</i>	Outlet
<i>s</i>	Solid

Drying of ground solids in a fluidized bed dryer has three characteristic zones namely: the warm-up, constant and falling drying rate zones [3]. In the warm-up zone, the solids immediately in contact with drying medium tend to approach steady state. Thus, resulting in either decrease or increase of drying rate [4]. At constant rate drying there is enough of the solvent to saturate the solids [5]. Towards the termination of the constant rate period is the critical solvent and transition to third characteristic zone (falling rate period). Drying takes longer time and less solvent is transferred due to internal resistances [4, 6]. Numerous models are available for predicting the drying rates in fluidized beds [7, 8].

Drying kinetics is crucial for effective process modelling and design, but the available data in literature are rarely sufficient for process design [8]. Espinosa *et al* [2] presented the experimental data for a fluidized bed dryer that was used to recover the solvents at three different temperatures of 40, 60 and 80°C. In their work, Espinosa *et al* [2] used two types of batch fluidized bed dryer to experimentally study the drying of hexane and ethanol from the neem seeds. The ground neem seeds were wetted separately with hexane and ethanol. The main objective of this work is to present a mathematical model for simulating the drying characteristics and the temperature distribution in a fluidized bed dryer. The proposed model is then validated using the experimental data from Espinosa *et al* [2].

2. Mathematical Model

Assuming that the solid particles are regarded as spherical, the heat loss to the surroundings is negligible and the gradients of concentration, temperature and pressure are ignored, the mathematical models, which describe the interchange of mass and energy between the solid and gas phases, are as presented below:

Unsteady state mass balance for the solid and gas phases are:

$$m_s \frac{dX}{dt} = -N_v \cdot A \quad (1)$$

$$\frac{dN_v}{dt} = -k'N_v \quad (2)$$

$$G(Y_{out} - Y_{in}) = N_v \cdot A \quad (3)$$

$$N_v = f(X)N_w \quad (4)$$

$$N_w = h_D C_T M (y_s - y_g) \quad (5)$$

Unsteady state energy balance for the solid and gas phases are:

$$m_s C_p \frac{dT_s}{dt} = A (q_c - N_v \cdot \lambda_{solvent}) \quad (6)$$

$$G(Cp_{g,out} T_{out} - Cp_{g,in} T_{in}) = -A \cdot q_c \quad (7)$$

$$q_c = h_c (T_g - T_s) \quad (8)$$

Integrating Eq. (1) at initial condition, $X = X_0$, gives the drying time,

$$t = -\frac{m_s}{N_w \cdot A} \int_{X_0}^X \frac{dX}{f(X)} \quad (9)$$

where $f(X)$ is the normalized drying rate describing the drying characteristics [9].

Also, integrating Equation (2) at initial condition, $N_v = N_{v0}$ gives the drying rate in terms of time.

$$N_v = N_{v0} \text{EXP}(-k' \cdot t) \quad (10)$$

Substituting Equation (10) in Equation (6) and integrating, at the initial condition, $T = T_{s0}$, gives the temperature distribution in the solid,

$$T_s = T_{s0} \text{EXP}\left(-\frac{Ah_c}{m_s C_p} t\right) + T_g \left(1 - \text{EXP}\left(-\frac{Ah_c}{m_s C_p} t\right)\right) + \frac{N_{v0} A \lambda}{h_c A - k' m_s C_p} \left[\text{EXP}\left(-\frac{Ah_c}{m_s C_p} t\right) - \text{EXP}(-k' t)\right] \quad (11)$$

A close look at Equations (9) and (11) will reveal that $f(X)$, h_c , h_D , N_{v0} and k' as well as the physical properties of air and solvent must be specified. Generally, normalized drying rate [9-11] is defined as follows:

$$f(X) = 1.0 - \text{EXP}(-N_{tG}) \quad (12)$$

where, N_{tG} is the number of gas transfer units in the bed. Hodges [10] approximates it as,

$$N_{tG} = \left(\frac{X}{a}\right)^b \quad (13)$$

where a and b are constants.

Alternatively, N_{iG} could be approximated by a polynomial function,

$$N_{iG} = c_0 + c_1X + c_2X^2 + c_3X^3 + \dots + c_nX^n \quad (14)$$

where c 's and n are coefficients and order of the polynomial respectively.

The heat transfer coefficient, h_C , is calculated from the equation:

$$Nu = p Re^r \cdot Pr^{1/3} = \frac{h_c d_s}{K} \quad (15)$$

$$h_c = \left(p Re^r Pr^{1/3} \right) \left(\frac{K}{d_s} \right) \quad (16)$$

where Nu is the Nusselt number, Re is the Reynolds number, Pr is the Prandtl number, p and r are the correlation constant and exponent respectively.

The mass transfer coefficient, h_D , is calculated using the Chilton-Colburn analogy [2],

$$h_D = \left(\frac{h_c}{C_p \cdot \rho} \right) \left(\frac{C_T}{C_{BLM}} \right) \left(\frac{Pr}{Sc} \right)^{2/3} \quad (17)$$

C_T is given by,

$$C_T = \frac{1}{V} = \frac{P}{RT} \quad [mol/m^3] \quad (18)$$

The gas bulk mean concentration, C_{BLM} , is expressed as [12],

$$C_{BLM} = \left[\frac{(1-y_g) - (1-y_s)}{\ln \left(\frac{1-y_g}{1-y_s} \right)} \right] C_T \quad (19)$$

The vapour fraction at solid and gas phases are defined as,

$$y_s = \frac{VP_{solvent}}{P} \quad (20)$$

where VP is the vapour pressure.

Since the solvent is not present in the drying medium, $y_g = 0$

The vapour pressure of the solvents at the solid surfaces are expressed by Antoine's equation [13],

$$\ln(VP_{Ethanol}) = 16.19 - \frac{34324}{T - 55.72} \quad (21)$$

$$\ln(VP_{Hexane}) = 13.982 - \frac{2744}{T - 45.93} \quad (22)$$

The latent heat of vaporisation of solvent (ethanol and hexane) is expressed as linear function of their corresponding temperature at melting and boiling points [14].

$$\lambda_{Ethanol} = -486551.020 + 3811.2245T \quad (23)$$

$$\lambda_{Hexane} = -52963.4146 + 1140.2439T \quad (24)$$

Also the physical properties of air (heat capacity, density, viscosity and thermal conductivity) as a function of temperature were obtained from Welty *et al* [12] in tabular form. The physical properties data were fitted with a polynomial using Microsoft Excel. The order of the polynomial was varied from 1 to 5 and the corresponding correlation coefficient (R^2) obtained. The polynomial with the highest R^2 is used for the computations.

As mentioned in the introduction the experimental data were obtained from Espinosa *et al* [2]. These data and other relevant inputs are summarized in Tables 1, 2 and 3.

Table 1. Physical Properties of Neem Seeds.

Description	De-oiled seed	Exhausted seed
	Large	Large
Weight Mean Diameter, 10^{-03} m	0.98	0.96
Average Density, kg/m^3	820	690
Exposed Area per Dry Mass, m^2/kg	7.51	9.11

Data source: Espinosa *et al* [2].

Table 2. Data Used for Drying of Neem Seed Treated with Hexane.

$T_{g,in}$ ($^{\circ}\text{C}$)	T_{s0} (K)	m_s (kg)	u_g (m/s)	X_0 (kg/kg)
40	274	0.890	0.80	0.530
60	289	0.853	0.85	0.470
80	285	0.799	0.90	0.500

Data source: Espinosa *et al* [2].

Table 3. Data Used for Drying of Neem Seed Treated with Ethanol.

$T_{g,in}$ ($^{\circ}\text{C}$)	T_{s0} (K)	m_s (kg)	u_g (m/s)	X_0 (kg/kg)
40	284	0.657	0.96	0.843
60	291	0.737	0.99	0.750
80	295	0.579	1.05	0.900

Data source: Espinosa *et al* [2].

A Fortran 77 programme was written to solve the model Eqs. (9) and (11).

3. Results and Discussion

The best polynomials that fitted the physical properties of air are shown in Table 4. These correlations are valid for the temperature range 290 to 370 K. Except for the heat capacity data with a correlation coefficient of 0.9999, the correlation coefficients

for other properties are 1.0000. This means that the polynomials fit the physical property data for air very well.

Table 4. Correlations for Heat Capacity, Density, Viscosity and Thermal Conductivity of Air.

Property	Correlation	R ²
Heat Capacity, J/kgK	$C_{p\text{ Air}} = 1021.6 - 0.1447T + 0.0003T^2$	0.9999
Density, kg/m ³	$\rho_{\text{ Air}} = 3.2381 - 0.0099T + 1 \times 10^{-05} T^2$	1.0000
Viscosity	$\mu_{\text{ Air}} = 1 \times 10^{-06} + 7 \times 10^{-08} T - 3 \times 10^{-11} T^2$	1.0000
Thermal Conductivity W/m.K	$K_{\text{ Air}} = 0.0003 + 1 \times 10^{-04} T - 3 \times 10^{-08} T^2$	1.0000

The experimental data was correlated assuming the Hodges' Equation, Eq. (13), and a polynomial function, Eq. (14). The results are shown respectively in Tables 5 and 6. These Tables indicate that, for a given solvent and temperature, the polynomial function gave a higher correlation coefficient than power law equation by Hodges [10]. Consequently equation 14 was used for the computation of drying rate.

Table 5. Correlation constants for Hodges Equation.

Solvent	Temperature (°C)	a	b	R ²
Hexane	40	0.2172	1.5218	0.9435
	60	0.1787	1.8425	0.9774
Ethanol	40	0.2523	1.4925	0.9670
	60	0.2245	0.7729	0.9731
	80	0.4231	1.3570	0.9527

Table 6. Correlation constants for Polynomial Function- Eq. (14)

Solvent	Temp (°C)	c ₀	c ₁	c ₂	c ₃	c ₄	c ₅	R ²
Hexane	40	-0.0005	-1.5000	121.18	-598.84	1084.4	-647.1	0.9820
	60	-0.0160	-1.7998	120.94	-542.67	777.34	-	0.9882
Ethanol	40	0.3168	-15.936	201.87	-648.83	848.66	-390.8	0.9882
	60	0.0757	-2.997	45.194	53.997	24.803	-	0.9818
	80	-0.0422	2.6369	-10.417	72.310	-151.63	94.861	0.9899

The values of the initial drying rate (N_{v0}) and the drying rate constant (k') are presented in Table 7. From this Table it can be seen that the drying constant increases

with temperature. This is in agreement with Arrhenius theory on the variation of rate constant with temperature [15, 16].

Table 7. Drying Kinetics (Drying Characteristics)

Solvent	Temperature (°C)	N_{v0} (kg/m ² sec)	k' (sec ⁻¹)
Hexane	40	0.0003	0.0049
	60	0.0004	0.0073
Ethanol	40	0.0001	0.0010
	60	0.0001	0.0012
	80	0.0003	0.0020

Figures 1 and 2 depict the drying rate curve and the temperature distribution for Hexane treated solids whilst those for Ethanol treated solids are shown in Figures 3 and 4. In these figures the experimental values are shown as symbols while the model predictions are shown as solid lines. At low solvent content ($X < 0.4\text{kg/kg}$) the model prediction is not very accurate especially for the ethanol treated solids. Otherwise the model fairly predicts the experimental data adequately. Except for hexane treated solid at 60°C, the model under predicts the solid temperature for time less than 500 seconds. At higher values of time, the model prediction is fairly accurate; the level of accuracy increasing as the time increases. The temperature curves (Figs. 2 and 4) also showed an initial drop. According to Espinosa et al [2] this is an indication of fast rate of drying. Within this region the model prediction is not very accurate.

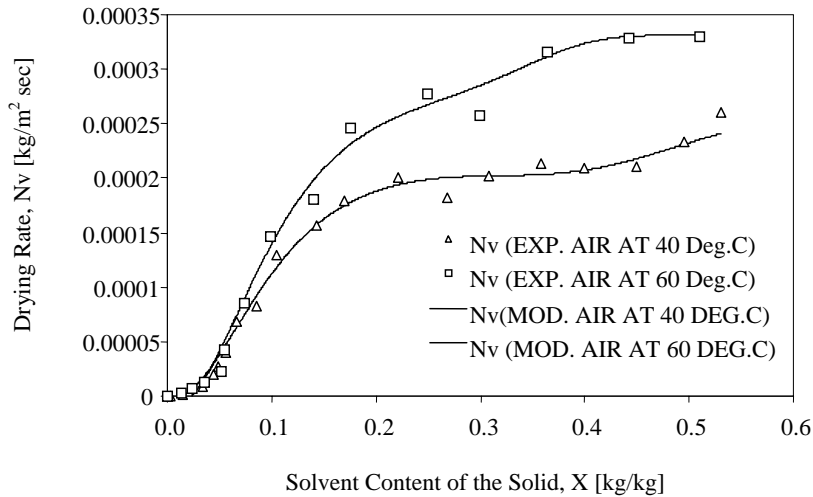


Fig.1. Drying Rate Curve of Hexane Treated Solids.

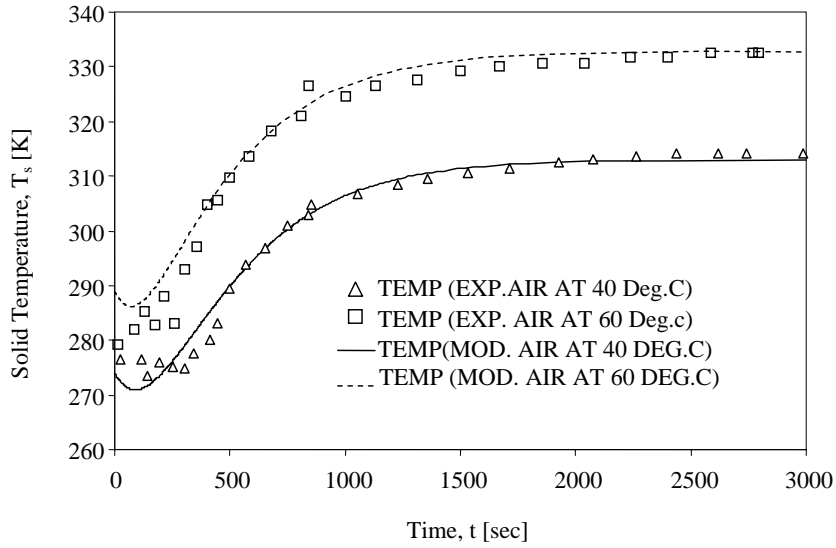


Fig. 2. Temperature Curve of Hexane Treated Solids.

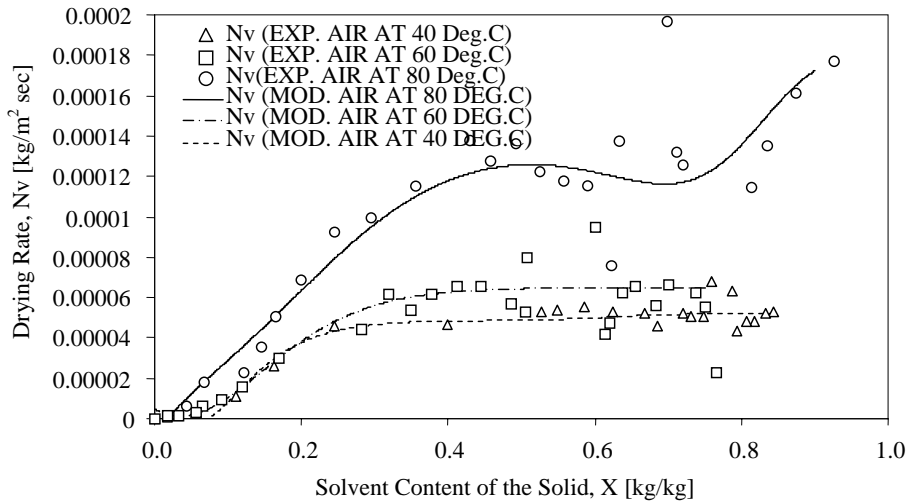


Fig. 3. Drying Rate Curve of Ethanol Treated Solids.

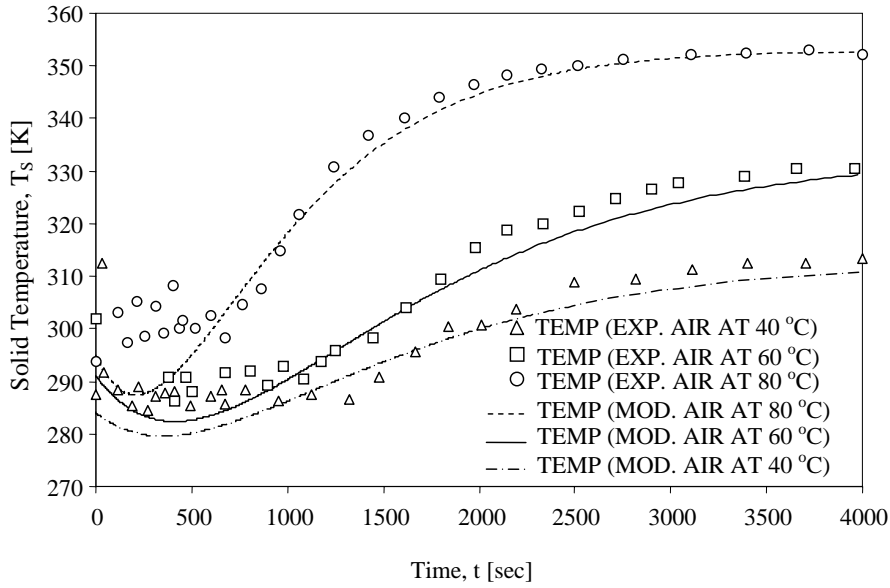


Fig.4. Temperature Curve of Ethanol Treated Solids

4. Conclusions

A model for simulating the drying of neem seeds in a fluidised bed has been presented. Before solving the model equations, the physical property data for air (specific heat, viscosity, density and thermal conductivity) as well as the number of gas transfer in the bed were fitted with a polynomial. The drying simulation results show that there was a good agreement between the experimental values and the corresponding model predictions except during the initial period.

References

1. Schmutterer, H. (1995). The neem tree *azadirachta indica* a. juss. and other meliaceae plants: Source of unique natural products for integrated pest management, medicine, industry and other purposes. *VCH Verlagsgesellschaft, Weinheim*, 326-365.
2. Espinosa, R., Lagerstedt, J., Nyman, T. & Martinez, J. (2002). Drying of ground neem seeds in a fluidized bed dryer. *Proceedings of the 13th International Drying Symposium (IDS' 2002)*, Beijing, China, vol. B, 1360.
3. Traub, D.A. (2003). The drying curve. *Process Heating Magazine*. Business Publishing Co., part 2.

4. Foust, S.A., Wenzel, L.A., LUMP, C.W. & Anderson, L.B. (1980). *Principles of Unit Operations* (2nd ed.). New York: John Wiley & Sons.
5. Butler, W. H. & Clark, D. (2000). Cascade vertical drying. *Proceedings of 12th International Drying Symposium (IDS 2000)*, No. 41, 1 – 10.
6. Coulson, J.M., Richardson, J.F., Backhurst J.R. & Harker, J.H. (1991). *Chemical Engineering*, vol. 2 (4th ed.). Oxford: Pergamon Press.
7. Peglow M., S. Heinrich, E. Tsotsas & L. Mörl (2004). Fluidized bed drying: influence of dispersion and transport phenomena. *Proceedings of the 14th International Drying Symposium (IDS 2004)*, São Paulo, Brazil, 22-25 August, vol. A, 129-136
8. Maroulis, Z. B. & Saravacos, G. D. (2002). Modelling, simulation and design of drying processes. *Proceedings of the 13th International Drying Symposium*, vol. A, 38.
9. Stenzel, M., Motta Lima, O.C., Pereira, N.C. & Mendes, E.S. (2003). Generalization of drying curves in conductive/convective drying of cellulose. *Braz. J. Chem. Eng.*, 20 (1), 81 - 86.
10. Hodges, C.R. (1982). Laboratory drying study and applications for paper machine drying. *Drying'82*, 99-105.
11. Treybal R.E. (1980). *Mass-Transfer Operations* (3rd ed.). Auckland: McGraw-Hill, Inc.
12. Welty, J. R., Wicks, C. E. & Wilson, R. E. (1976). *Fundamentals of Momentum, Heat and Mass Transfer* (2nd ed.). New York: John Wiley & Sons.
13. Isidoro, M. (2003). Vapour Pressure of Solvents, <http://imartinez.etsin.upm.es/dat1/ePV.htm>
14. Isidoro, M. (2003). Liquid Properties. <http://imartinez.etsin.upm.es/dat1/eLIQ.htm>
15. Octave L. (1988). *Chemical Reaction Engineering*. New Delhi: Wiley Eastern Ltd.
16. Susu, A. A. (1997). *Chemical Kinetics and Heterogeneous Catalysis*. Nigeria: CJC Press Ltd.